

PAPER • OPEN ACCESS

Applicability of zirconium loaded okara in the removal and recovery of phosphorus from municipal wastewater

To cite this article: T A H Nguyen *et al* 2019 *IOP Conf. Ser.: Earth Environ. Sci.* **266** 012004

View the [article online](#) for updates and enhancements.

Applicability of zirconium loaded okara in the removal and recovery of phosphorus from municipal wastewater

T A H Nguyen¹, H H Ngo², W S Guo², T Q Pham³, T H Cao⁴ and T H H Nguyen⁴

¹ Master's Program in Environmental Engineering, VNU Vietnam Japan University, Luu Huu Phuoc, My Dinh 1 residential area, Nam Tu Liem, Hanoi, Vietnam

² Centre for Technology in Water and Wastewater, School of Civil and Environmental Engineering, University of Technology, Sydney (UTS), 15 Broadway, Ultimo, NSW 2007, Australia

³ Graduate University of Science and Technology, Vietnam Academy of Science and Technology, 18 Hoang Quoc Viet, Cau Giay, Hanoi, Vietnam

⁴ Faculty of Geology, VNU University of Science, 334 Nguyen Trai, Thanh Xuan, Hanoi, Vietnam

E-mail: nta.hang@vju.ac.vn

Abstract. Recently, there is a new trend to consider wastewater as a precious resource. Since phosphorus is a limited non-renewable element, and MAP (Magnesium Ammonium Phosphate - $\text{MgNH}_4\text{PO}_4 \cdot 6\text{H}_2\text{O}$) is a valuable slow-release fertilizer, the recovery of phosphorous as MAP has received special attention from scientists all over the world. However, the application of this process with municipal wastewater is still a challenge, due to low concentration of phosphorus and high volume of municipal wastewater. This study investigates the potential of reclaiming MAP from municipal wastewater by combination of adsorption and crystallization. Soybean milk residue (okara) was loaded with Zirconium (Zr) to prepare the adsorbent (ZLO). Adsorption and desorption experiments were conducted in a semi-pilot scale ZLO packed column system. Effects of P: N: Mg molar ratios, chemical sources and temperature on the formation of MAP were examined in an attempt to identify the optimal crystallization conditions. The attained precipitate was characterized using XRD, SEM, FTIR techniques. It was found that the ZLO packed column adsorption-desorption system could pre-concentrate phosphorus from municipal wastewater up to 28.36 times, fitting well the minimum requirement (50 mg P/L) for the economical MAP recovery. Up to 95.19% of dissolved phosphorus in desorption solution was recovered at pH = 9, Mg: N: P molar ratio = 2:2:1, using a combination of $\text{MgCl}_2 \cdot 6\text{H}_2\text{O}$ and NH_4Cl . The harvested MAP exhibited high purity (92.59%), high P-availability (89% by mass), and extremely low levels of heavy metals. The results prove that it is viable to recover MAP from municipal wastewater by employing ZLO as adsorbent, followed by crystallization. This paves the way for mining phosphorus from municipal wastewater and reducing okara as an agricultural byproduct in a green way.

1. Introduction

1.1. The significance of phosphorus removal and recovery

Phosphorus plays a vital role in the development of living organisms. It is known as one of essential elements for the plant growth [1]. It is also a key component of deoxyribonucleic acid (DNA),



ribonucleic acid (RNA), adenosine triphosphate (ATP), phospholipids, teeth and bones in animal bodies [2]. Additionally, phosphorus is a fundamental material of many principal industries, such as fertilizers, detergents, paints, corrosion inhibitors, beverages, and pharmaceuticals [3]. Despite the irreplaceable role of phosphorus in the human daily life, the global phosphate rock reserves can be depleted in 50-100 years [4]. In another perspective, the excessive amount of phosphorus can induce eutrophication in water bodies. To protect the surface water from this undesired phenomenon, the phosphorus concentration in effluents should range between 0.5 and 1 mg P/L before discharging into aquatic medium [5]. Consequently, an appropriate treatment technology is required to meet the stringent regulation [6]. For these reasons, the removal and recovery of phosphorus from wastewater have recently become a matter of urgency.

1.2. The potential and challenges of recovering phosphorus from municipal wastewater

The municipal wastewater can be a potential source for phosphorus recovery, due to the enormous volume regenerated worldwide and low levels of hazardous substances. However, the main challenge to the phosphorus recovery from municipal wastewater that currently exists is the low concentration of phosphorus [7]. It is observed that the concentration of total phosphorus in municipal wastewater is varying, such as 4.2 mg/L [8], 4-15 mg/L [9], [10], 8-10 mg/L [5], 10 mg/L [2], [11], [12]. Since orthophosphate normally accounts for approximately 50% of the total phosphorus, the concentration of orthophosphate in municipal wastewater is usually limited to 15 mg/L [2], [5], [11], [12], [13]. However, the phosphorus level of the aqueous solutions above 50 mg P/L is required to ensure an economical MAP recovery [14]. Meanwhile, it is well-documented that adsorption has significant advantages that can favor phosphorus recovery, such as suitability for the treatment of diluted wastewater, high selectivity in presence of foreign anions, high potential of phosphate pre-concentration, and production of a reusable phosphorus [15], [16]. Hence, it is assumed that the combination of adsorption and crystallization may be a solution for MAP recovery from municipal wastewater.

1.3. Significance of using agricultural waste/by-products based adsorbents for phosphorus removal and recovery

Agricultural waste/by-products (AWBs) have several properties that make them attractive as the substrate for developing phosphorus adsorbents. To begin, AWBs are abundant, low-priced, and non-toxic. In addition, AWBs usually have chemical stability and high reactivity. Particularly, AWBs have appropriate chemical composition (cellulose, hemicelluloses) with a large number of active hydroxyl groups. Consequently, AWBs can easily be involved in chemical reactions for the preparation of functional groups of adsorbents, for example metal loading, polymerization, graft reaction [17]. It provides a foundation for AWBs to be converted into some functional polymers [18]. Specifically, the -OH groups can combine with alkoxyamine ligands, and hence enhancing their anion exchange abilities [19]. The use of AWBs as phosphorus adsorbents may result in many benefits. Firstly, it can protect surface water from eutrophication. Secondly, the recycling of AWBs as phosphate adsorbents not only provides a viable solution to reduce waste materials in a cheap and eco-friendly way but also adds value to AWBs [4], [20], [21]. In addition, the production of anion exchange resins from abundant, cheap and renewable AWBs may help reduce the cost of phosphorus treatment. Moreover, by converting phosphorus in wastewater into fertilizers, this practice can generate revenues [22]. Clearly, the use of AWBs based adsorbents for phosphorus removal and recovery may provide a sustainable, efficient and profitable solution for phosphorus pollution management.

1.4. Soybean by-product (okara) as a choice medium

Okara is a byproduct of soy beverage and tofu production. It has a white color and is quite similar to wet sawdust in its texture and form. Okara is also named as soybean milk residue, soy pulp, soy fines, bean mash, bean curd dreg (English), le okara (French), das okara (German), tofuzha or douzha (Chinese), tofukasu (Japanese), bejee (Korean), sepal (Filipino), ampastahu (Indonesian), tauhu tor (Thai). Okara was chosen for investigation in this study because it is insoluble in water, non-toxic, cheap,

easy acquiring and abundantly available. As a by-product of food processing, okara is clean and can be used directly as a water treatment material. Moreover, due to the existence of large amounts of hydroxyl and carboxyl groups on its cell walls, okara can easily and efficiently involve in chemical modification reactions [18]. Although soybean by-products were used for the adsorption of organochlorine compounds, benzene, heavy metals, and reactive dye from aqueous solutions, okara has never been investigated for the removal and recovery of phosphorus.

1.5. Research gaps

Although phosphorus can be removed from wastewater by a wide range of technologies, there is still lack of a process that can not only remove but also recover phosphorus in a sustainable form [23]. To date, very little work has been done on the beneficial use of AWBs based adsorbents for phosphorus recovery [24]. So far, phosphorus has been successfully recovered from many kinds of phosphorus rich wastewater, such as swine wastewater [25], [26], eutrophic water [15], sludge liquor [23], [27], membrane concentrate [28]. However, the MAP recovery from desorption solution has rarely been tested [29].

1.6. Objectives of the study

The goal of this study was to investigate the feasibility of recovering phosphorus as MAP from municipal wastewater using adsorption followed by crystallization. To overcome a challenge, which is low concentration of phosphorus in municipal wastewater, adsorption test using ZLO was applied to pre-concentrate phosphorus in desorption solution in advance. The effect of solution pH, Mg: N: P molar ratio, chemical type, and reaction temperature on MAP crystallization was examined. The recovered MAP was characterized using XRD, SEM, FTIR, elemental analysis, and P-bioavailability. This research is expected to provide a novel and viable technique for reclaiming phosphorus from municipal wastewater and reducing soybean waste in an eco-friendly way.

2. Materials and methods

2.1. Materials

2.1.1. Zirconium loaded okara (ZLO) as a phosphorus biosorbent. The fresh okara was collected from Nhu Quynh tofu and soy milk workshop, Yagoona, New South Wales, Australia. It was then dried in the oven at 105 °C for 24 h for a long use. After being cooled down to the ambient condition, the dried okara was kept in plastic bags for chemical treatments.

Since raw okara could hardly remove phosphate from aqueous solutions, a chemical modification of okara was applied to enhance its phosphate removal efficiency. In a previous study, three categories of phosphate biosorbents were developed from okara using metal loading method, including iron (Fe^{3+}) loaded okara (ILO), iron/zirconium ($\text{Fe}^{3+}/\text{Zr}^{4+}$) loaded okara (IZLO) and zirconium loaded okara (ZLO). Among three developed biosorbents, ZLO proved to be superior to IZLO and ILO, with respect to adsorption, desorption, regeneration and metal leaching [30]. Consequently, ZLO was selected for next experiments. The modification method was then further optimized. Three modification conditions were tested to evaluate the effect of varying the concentration of NaOH and Zr^{4+} solutions on the phosphate removal efficiency of the biosorbents. Considering the economic and technical feasibility, the combination between 0.05 M NaOH and 0.25 M Zr^{4+} solution was regarded as the optimal modification condition. Therefore, ZLO produced at this modification condition will be used in this study. The detailed procedure for the development of ZLO can be detected in another technical paper [31].

2.1.2. Municipal wastewater. The raw municipal wastewater was sampled from Sydney Olympic Park Water Treatment Plant, Australia. After being settled for 24 h, the raw wastewater was screened through a 150 μm stainless steel sieve and used for adsorption tests.

2.1.3. Chemical reagents. The chemicals used in this work were of analytical grade. The solutions of 0.05 M and 0.2 M NaOH, 0.1 M HCl and 0.25 M $\text{ZrOCl}_2 \cdot 8\text{H}_2\text{O}$ were prepared by liquefying proper amounts of sodium hydroxide (NaOH), hydrochloric acid (HCl), and zirconyl chloride octahydrate ($\text{ZrOCl}_2 \cdot 8\text{H}_2\text{O}$) in the milli-q water.

2.2. Methods

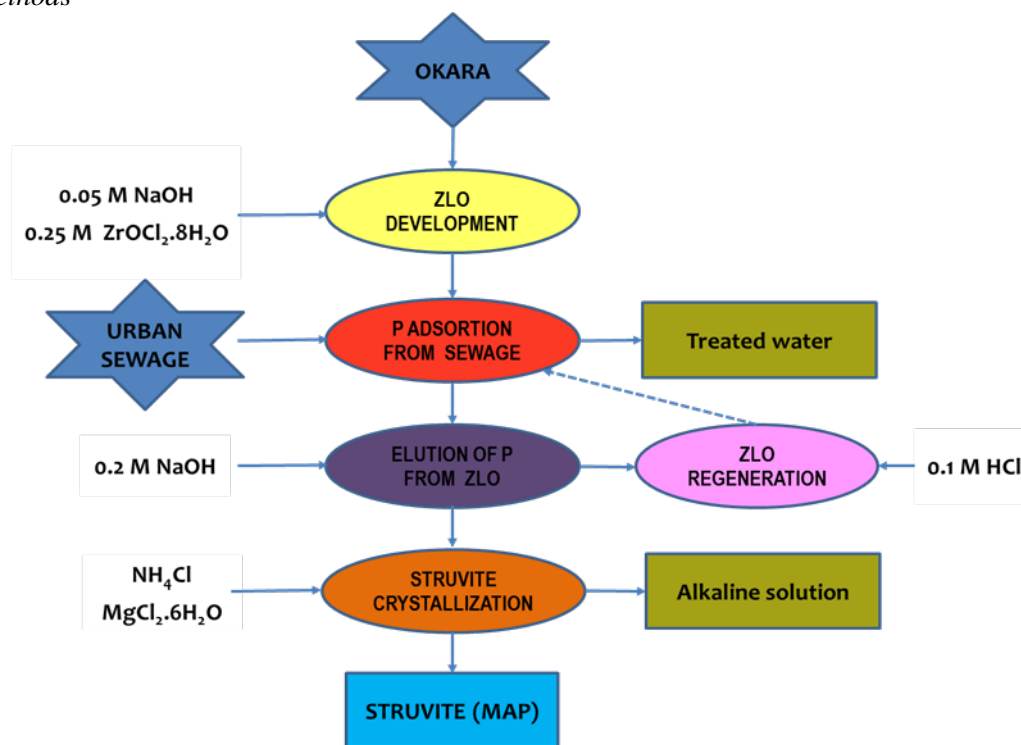


Figure 1. The experimental set-up.

2.2.1. Phosphorus adsorption and elution. The dynamic adsorption test was conducted using a big-scale glass column (4.5 cm internal diameter \times 120 cm height). The raw municipal wastewater was percolated through the column in the upward direction at a flow rate of 53 mL/min using a peristaltic pump (Masterflex® Console Drive, Model No. 77521-47, Cole-Parmer Instrument Company). The investigation shows that ZLO has a relatively low density (1.15 g/cm^3) and a high porosity (68.70%). Therefore, ZLO is assumed to be appropriate for being applied in the packed bed column in the upward direction. The column was washed every 24 h in the upward direction at a flow rate of 200 mL/min for 30 min each time to prevent water clogging. The flow was applied in upward direction with the conditions that a sieve on the top of the column was taken out in advance. When the water level inside the column nearly reached the column outlet, it was withdrawn from the bottom of the column. By that way, the ZLO bed moved up and down continuously in the column. The solids were moved to the top of the bed and got out of the column with the cleaning water. Consequently, the water clogging was improved. To prevent ZLO from getting out of the column, a sieve on a bucket was put at the end of the outlet tube. The spilled ZLO was then packed into the column again to ensure the minimal weight loss of ZLO.

The effluent samples were collected at pre-determined intervals in 14 mL plastic tubes for the phosphorus analysis. After adsorption, the ZLO bed was rinsed with the tap water at a flow rate of 53 mL/min for 1 h to remove the residual phosphorus from adsorption test. Then the elution test was carried out using 0.2 M NaOH at a flow rate of 13.24 mL/min for 5 h. This flow rate was selected since the test demonstrated that it ensured enough contact time between P laden ZLO and elution solution, and thus resulting in high desorption efficiency. The effluent samples were collected in a 14 mL plastic tube for

measurement of phosphorus and other quality parameters. After desorption, the exhausted ZLO bed was taken out of the column, washed with tap water, and activated with 1 L of 0.1 M HCl for 3 h. After desorption test, some OH⁻ anions can be left on the surface of ZLO. This may lead to a reduction in the PO₄³⁻ adsorption capacity of ZLO in the next cycle, due to the competition between residual OH⁻ on the surface of ZLO and PO₄³⁻ in aqueous solution for anion binding sites on the surface of ZLO. Washing ZLO with tap water enables the removal of residual OH⁻ ions while activating ZLO with 0.1 M HCl helps produce the appropriate pH condition for the next adsorption test. After being washed with the tap water, the activated ZLO was packed into the column again for the next adsorption cycle.

The eluted amount of phosphorus (EAP) is calculated by the following equation [32]:

$$\text{EAP (mg/g)} = (1/m) \sum_{q=1}^{n2} C_q V_q \quad (1)$$

where C_q , V_q , and $n2$ are the effluent phosphorus concentration, volume of the q -th fraction, and number of the last fraction in the desorption experiment.

2.2.2. MAP crystallization. In this work, a glass 2 L beaker was used as the crystallization reactor in this study. The phosphorus source for MAP crystallization in this work was desorption solution. The MAP crystallization tests were performed to evaluate the effect of solution pH (9.0, 9.5, and 10.0). Three different P: N: Mg molar ratios (1:1:1, 1:1.5:1.5, and 1:2:2) were investigated. In addition, the MAP crystallization was evaluated using different chemical sources (NH₄Cl + MgCl₂·6H₂O and (NH₄)₂SO₄ + MgSO₄·7H₂O). The influence of solution temperature (281 and 295 K) on the MAP crystallization was also examined. To ensure a steady phosphorus concentration, desorption solution was accumulated to an adequately large volume, and then was divided equally. First, desorption solution was vigorously stirred at 200 rpm for 0.5 h to remove the dissolved CO₂. Second, the pH of desorption solution was adjusted to around 8 using H₂SO₄ 98% to prevent NH₃ evaporation or Mg precipitation when external sources of ammonium and magnesium were added. Third, NH₄Cl was added to desorption solution before MgCl₂·6H₂O to avoid the formation of magnesium phosphate. Then, the mixture was agitated at 120 rpm to dissolve NH₄Cl and MgCl₂·6H₂O entirely. Next, the pH of solution was raised to a desired value for MAP crystallization using 5 M NaOH. After that, the mixture was stirred at 120 rpm for 30 min, followed by settling for another 30 min. The suspension was used for the determination of residual PO₄³⁻, Mg²⁺, and NH₄⁺. The suspension was then filtered through 1.2 μm filter paper and the solid was washed with milli-q water seven times. Finally, the precipitate was dried in the oven at 40 °C for 24 h.

2.2.3. Elemental analysis. The elemental analysis of the harvested precipitate was conducted by the dissolution method [25], [33]. Accordingly, 0.2 g of the precipitate was dissolved in 10 mL of 32% hydrochloric acid and then diluted to 1 L with milli-q water. The mixture was stirred continuously at 200 rpm for 1 h prior to the analysis of Mg²⁺, NH₄⁺-N, and PO₄³⁻-P.

2.2.4. MAP purity evaluation. In this study, the MAP purity was evaluated by a method adapted from [33]. This method also includes two major steps as suggested by [33], which are (1) dissolution of the precipitate and (2) elemental analysis of the obtained solution. However, considering the fact that ammonium (NH₄⁺) compound used for the crystallization reaction may be left in the harvested precipitate, this study suggested that MAP purity be determined according to the minimum molar number of MAP components instead of NH₄⁺ molar number as proposed by [33].

2.2.5. The P-bioavailability. The P-bioavailability of the recovered precipitate was evaluated by its solubility in the 2% citric acid [29]. The solution was prepared by dissolving 0.3 g of the precipitate with 100 mL of 2% citric acid in a glass flask. The flask was placed on a flat shaker at a speed of 120 rpm for 2 h at room temperature. After filtration with 1.2 μm filter paper, the solution was utilized for phosphorus measurement.

2.3. Analytical methods and instrumentation

2.3.1. Characterization of municipal wastewater, desorption solution, and effluent. Phosphate ($\text{PO}_4\text{-P}$), nitrate ($\text{NO}_3\text{-N}$), and ammonium ($\text{NH}_4\text{-N}$) parameters were analyzed using Spectroquant NOVA 60, Merck (Germany). Magnesium (Mg^{2+}), calcium (Ca^{2+}), zirconium (Zr^{4+}), and heavy metals were determined by 4100 MP-AES Spectrometer (Microwave Plasma-Atomic Emission Spectrometry), Agilent Technologies (USA). The pH was measured by Hach HQ40d Multi meter. The chemical oxygen demand (COD) analysis was carried out with Hach DR/2000 Spectrophotometer. The total suspended solids (TSS) were determined in accordance with the standard method.

2.3.2. Characterization of the precipitate. The crystal structure was characterized by Siemens D5000 X-ray Diffractometer (XRD). The morphology was examined by Zeiss Evo LS15 SEM (Germany). The FTIR pattern was recorded on an IRAffinity-1 Fourier Transform Infrared Spectrophotometer, Shimadzu Corporation (Japan).

3. Results and discussion

3.1. Phosphorus pre-concentration

The municipal wastewater used in this study had a mean concentration of 5.5 mg P/L. It was far too low when compared to 50 mg P/L, the recommended minimum level for an economical MAP recovery. Therefore, this study investigates the phosphorus pre-concentration by adsorption - desorption processes in a semi pilot-scale ZLO packed bed column.

In the adsorption test, a big column (4.5 cm x 120 cm) was packed with 100 g of ZLO. The municipal wastewater with the phosphorus concentration of 5.5 mg P/L was percolated through the column in the upward direction with the flow rate of 53 mL/min. The operating conditions of the column adsorption test were presented in Table 1. The breakthrough curve for phosphorus adsorption onto ZLO column was shown in Figure 2. It can be seen from the figure that the breakthrough occurred at 34.5 h while exhaustion was achieved at 109.7 h. The dynamic adsorption capacity of ZLO for phosphorus at the saturation time was 10.99 mg P/g ZLO, representing 70.34% its equilibrium adsorption capacity. The phosphate retention onto ZLO may occur due to electrostatic attraction between phosphate anions in the solution and Zr^{4+} ions onto ZLO surface [34].

Table 1. The adsorbent and big column properties in the dynamic adsorption test.

Parameter (Symbol)	Unit	Value
ZLO weight (m)	g	100
ZLO bed height (Z)	cm	30
ZLO bed volume (BV)	cm^3	477
P initial concentration (C_0)	mg/L	5.5
Volumetric flow rate (Q)	cm^3/min	53
Superficial velocity (V_s)	cm/min	3.33
Empty bed contact time (EBCT)	min	9

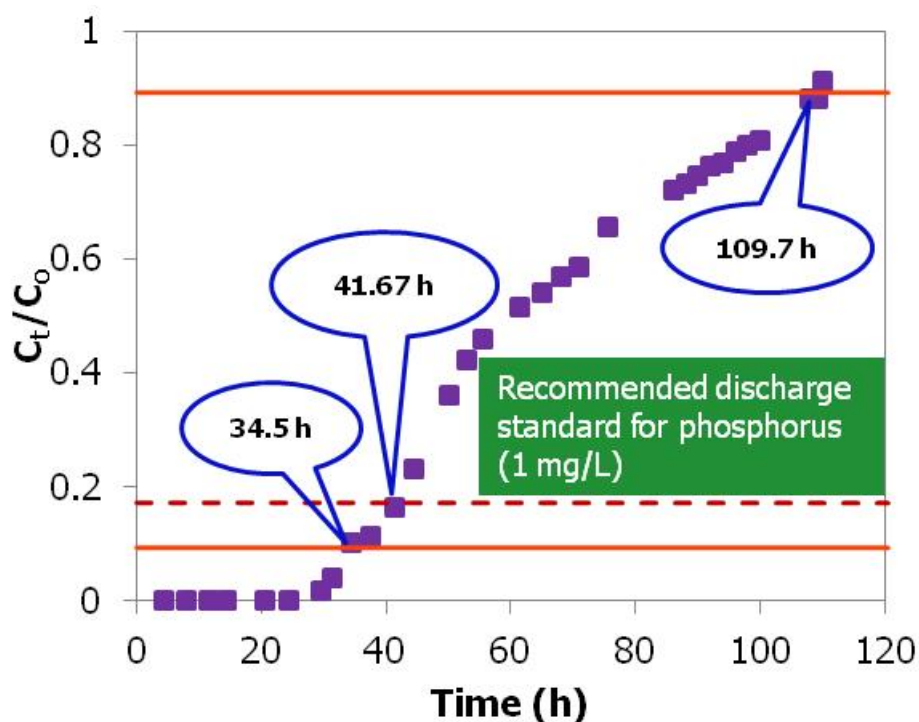


Figure 2. Breakthrough curve for phosphorus adsorption from real municipal wastewater on ZLO packed bed column at pilot scale (100 g ZLO; bed depth of 30 cm, flow rate of 53 mL/min, and influent phosphorus concentration of 5.5 mg/L).

Desorption test was performed by feeding 0.2 M NaOH solution through the bed in the upward direction. According to [35], a high concentration of phosphorus in the effluent could be obtained by applying a low flow rate for desorption test. To do that, the desorption test in this study utilized the flow rate of 13.24 mL/min, which was much lower than that for adsorption test (53 mL/min) but still ensured high desorption efficiency. Desorption profile was shown in Figure 3. As is illustrated by the figure, desorption of phosphorus from ZLO column was almost completed within 20 h, after which it was marginal. The phosphorus desorption efficiency at 20 h was 72.89%. The total volume and phosphorus concentration of the effluent at 20 h were 15.9 L and 50.36 mg/L, respectively. By using exhausted desorption, the phosphorus concentration in desorption solution was increased by 9.16 times compared to that in the influent. It was interesting to note that though desorption ended at 20 h, more than 80% of the eluted phosphorus could be attained by 5 h. The total volume and phosphorus concentration of the effluent at 5 h were 3.975 L and 156 mg/L, respectively. At this time, the phosphorus concentration in the desorption solution was 28.36 fold higher than that in the raw municipal wastewater. In view of phosphorus recovery, a desorption solution with a high concentration of phosphorus is desirable. Hence, it is highly recommended to finish desorption by 5 h.

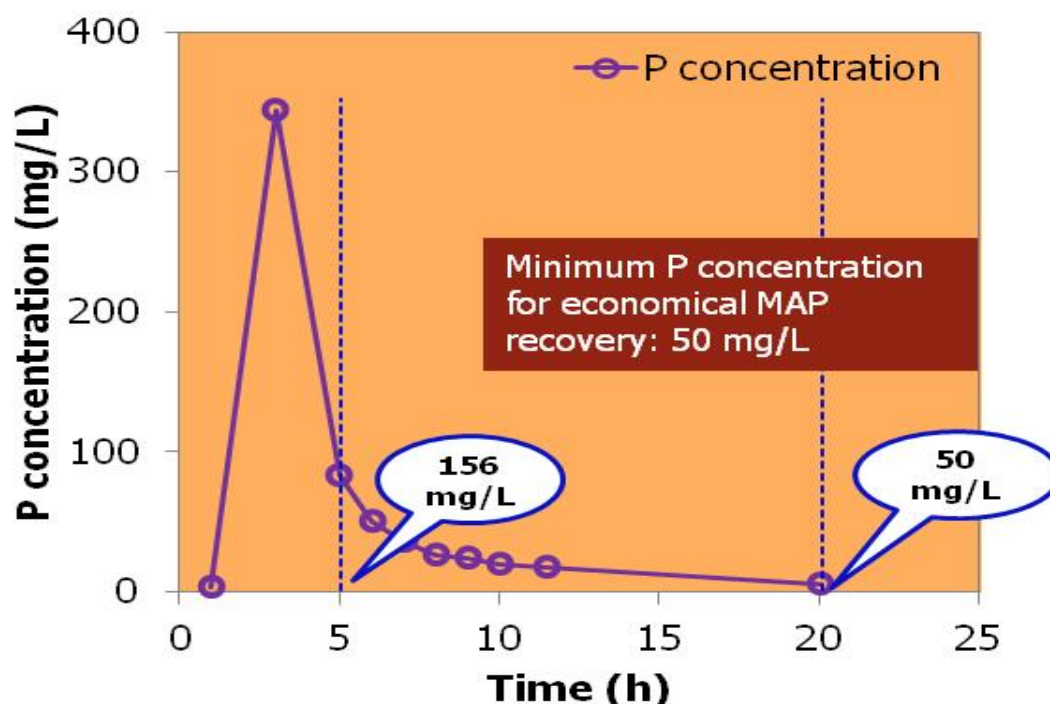


Figure 3. Desorption profile of ZLO packed bed column (100 g ZLO, desorption solution of 0.2 M NaOH, flow rate of 13.24 mL/min).

It was observed that it took a shorter time for 5 h eluted ZLO column to get saturated in the next adsorption cycle than 20 h eluted ZLO column. This can be attributed to the incomplete desorption of the former column. However, the amounts of desorbed phosphorus in these two columns were the same. The result proved that incomplete desorption had no significant impact on the next desorption cycles. Thus, it can be used as an effective means to achieve an adequately high phosphorus concentration for MAP recovery.

3.2. Phosphorus recovery as MAP from desorption solution

3.2.1. Characterization of desorption solution. The characterization of desorption solution is necessary as co-existing ions and the alkaline of desorption solution may affect the purity of the precipitate, and the alkali requirement for pH alteration in MAP crystallization [23]. The phosphorus concentration of the desorption solution was 156 mg/L, almost 28.36 times higher than that of raw municipal wastewater. Though NH_4^+ ions were present in desorption solution (9.4 mg/L), the $\text{NH}_4^+ : \text{PO}_4^{3-}$ molar ratio was still very low (1:7.45). It implied that there was a need to use additional source of NH_4^+ to ensure successful MAP crystallization. The existence of Mg^{2+} (0.9 mg/L) in desorption solution was expected to favor the MAP crystallization. Notably, the concentration of Ca^{2+} was 12.9 mg/L. Nevertheless, the Ca/Mg molar ratio when an external source of magnesium was added for MAP crystallization was 0.03. This ratio was still lower than the warning level (>0.5) that can impede the MAP crystallization [26]. However, due to the presence of Ca^{2+} in desorption solution, CaSO_4 can be formed instead of MAP if $(\text{NH}_4)_2\text{SO}_4$ and $\text{MgSO}_4 \cdot 7\text{H}_2\text{O}$ are used for crystallization [15]. This should be taken into consideration when the external sources of NH_4^+ and Mg^{2+} are selected. The concentration of TSS in desorption solution was 120 mg/L. This was far too low compared to the limit (1000 mg TSS/L) that may cause a significant effect on crystallization of Ostara Pearl® technology [36]. The level of NO_3^- in desorption solution was minor (2.7 mg/L). The Zr^{4+} ions could not be found in desorption solution. The levels of heavy metals in desorption solution were negligible. The pH of desorption solution (12.63) was much higher than that

of normal wastewaters (6.5-8.5) used for phosphorus recovery. This may lead to NH_3 evaporation and/or Mg precipitation when external sources of NH_4^+ and Mg^{2+} are added. Therefore, the pH of desorption solution should be reduced to below 8 in advance. Overall, high phosphorus concentration was an advantage, whereas high pH value can be cited as a drawback when desorption solution was used for MAP recovery.

3.2.2. Factors influencing the MAP recovery. The effect of pH on MAP crystallization was evaluated by using different solution pH (9, 9.5, and 10) while maintaining other crystallization conditions constant. It was found that the phosphorus recovery efficiency increased from 88.70 to 93.73% when pH rose in the range between 9 and 10. On the contrary, the MAP purity was reduced from 91.88 to 86.87% with the above pH augmentation. These findings are consistent with results reported by [33] and [15]. As the difference in the phosphorus recovery efficiency was not significant, and MAP was a favorite recovered product, the pH 9 was selected as the optimal pH and used for other crystallization experiments. This is supported by [36], who recommended recovering MAP at a lower pH value to mitigate the chemical costs. A similar optimal pH (9.0) was applied by [25] for MAP recovery from swine biogas digester effluent.

In order to evaluate the effect of Mg: N: P molar ratio on the MAP formation, three molar ratios (1:1:1, 1.5:1.5:1, and 2:2:1) were tested. The increase in the Mg: N: P molar ratio (from 1:1:1 to 2:2:1) led to the escalation of the P recovery efficiency (from 51.5 to 95.19%). On the contrary, it resulted in a slight reduction in the MAP purity. Especially, it had a considerable effect on the shape and size of MAP crystals. While MAP crystals were single and orthorhombic at the Mg: N: P molar ratio of 1:1:1, they were mostly aggregate and amorphous at the ratios of 1.5:1.5:1 and 2:2:1. In addition, the MAP crystals harvested at the lower molar ratio were longer in size (30-40 μm) than those obtained at the higher molar ratios (10-20 μm). Though the Mg: N: P molar ratio of 1:1:1 resulted in the highest MAP purity, the P recovery efficiency (51.5%) was far too low for any practical application. The MAP purity obtained at two remaining Mg: N: P molar ratios were quite similar (92.59% and 98.63%). However, the P recovery efficiency at the 2:2:1 molar ratio (95.19%) was much higher than that at the 1.5:1.5:1 molar ratio (88.69%). For these reasons, 2:2:1 was selected as the optimal molar ratio for MAP crystallization. The Mg: P molar ratio greater than 1:1 has been also used by many researchers, such as 1.4:1 [26], 2.0:1 [37] and 4.2:1 [38].

This study evaluated the effect of using two chemical combinations, which were $\text{NH}_4\text{Cl} + \text{MgCl}_2 \cdot 6\text{H}_2\text{O}$ and $(\text{NH}_4)_2\text{SO}_4 + \text{MgSO}_4 \cdot 7\text{H}_2\text{O}$, on MAP synthesis. It was found that the P recovery efficiency was decreased from 94.87 to 91.64% when the combination of $(\text{NH}_4)_2\text{SO}_4 + \text{MgSO}_4 \cdot 7\text{H}_2\text{O}$ was replaced by $\text{NH}_4\text{Cl} + \text{MgCl}_2 \cdot 6\text{H}_2\text{O}$. Moreover, the MAP purity when applying $\text{NH}_4\text{Cl} + \text{MgCl}_2 \cdot 6\text{H}_2\text{O}$ (81.97%) was higher than that of $(\text{NH}_4)_2\text{SO}_4 + \text{MgSO}_4 \cdot 7\text{H}_2\text{O}$ (77.79%). This can be explained by the fact that Ca^{2+} in desorption solution may react with SO_4^{2-} to form CaSO_4 as impurities. Additionally, the majority of MAP crystals had the same size, which averaged between 20 and 25 μm when NH_4Cl and $\text{MgCl}_2 \cdot 6\text{H}_2\text{O}$ was used. In contrast, the size of MAP crystals varied in a wider range from 5 to 35 μm when $(\text{NH}_4)_2\text{SO}_4 + \text{MgSO}_4 \cdot 7\text{H}_2\text{O}$ applied. Apparently, the combination of $\text{NH}_4\text{Cl} + \text{MgCl}_2 \cdot 6\text{H}_2\text{O}$ exhibited the better performance when compared to $(\text{NH}_4)_2\text{SO}_4 + \text{MgSO}_4 \cdot 7\text{H}_2\text{O}$. These results are consistent with those reported by [39].

The reaction temperature can affect the MAP crystallization through the MAP components activity and MAP crystals solubility [39]. This study investigated the difference in MAP crystallization when two different reaction temperatures were applied. It was observed that when the reaction temperature was augmented from 281 to 295 K, the P recovery efficiency and the MAP purity were reduced by 10.84% and 0.62%, respectively. The increase in reaction temperature slightly reduced the size of MAP crystals. This can be ascribed to a higher solubility product of MAP crystals at a greater temperature [40]. Similar observations were reported by [39]. However, in view of practical application, the room temperature (295 K) was selected as the ideal temperature for MAP crystallization.

Considering the P removal efficiency, MAP purity and practical applicability, the best condition for MAP crystallization was the solution pH of 9, the Mg: N: P molar ratio of 2:2:1, reaction temperature of 295 K, agitation speed = 120 rpm, and a chemical combination of $\text{MgCl}_2 \cdot 6\text{H}_2\text{O}$ and NH_4Cl .

3.2.3. Precipitate evaluation. The precipitate attained at the optimal condition was characterized by element, XRD, SEM, FTIR, and P-bioavailability analyses.

The main components of the harvested precipitate were determined by dissolution method followed by elemental analysis. The percentage by weight of P, Mg, and N in the recovered MAP were 11.96%, 9.07% and 5.48%, respectively. These values were quite similar to those for the standard MAP (Sigma), which were 12.65%, 9.80%, and 5.71%, correspondingly. The results confirmed that the MAP recovered from desorption solution had a high purity. According to [6], phosphate ores can be classified as low grade (up to 3 wt. % P), intermediate - grade (4-5 wt. % P), and high-grade (6-8 wt. % P). The recovered precipitate had 12.19 wt. % P, and thus can be placed among high-grade phosphate ores. The contents of Cu, Zn, Pb, Cd, Cr, and Ni in the reclaimed MAP were 5, 11, 3, 0.1, 1, and 1 ppm while the German legal limits were 70, 1000, 150, 1.5, 2, and 80 ppm, respectively. The comparison shows that the recovered MAP had a high purity.

XRD patterns of the recovered precipitate and the standard MAP are illustrated in Figure 4. As the figure shows, the XRD pattern of the harvested precipitate almost coincided with that of the standard MAP, ($\text{MgNH}_4\text{PO}_4 \cdot 6\text{H}_2\text{O}$), with respect to the position and intensity of the peaks. The result verifies that the obtained precipitate is mainly MAP crystals. A minor difference in the peak intensity between these two XRD patterns can be attributed to the presence of impurities in trivial quantities. Similar locations of the peaks of the recovered MAP were observed by [29], [39].

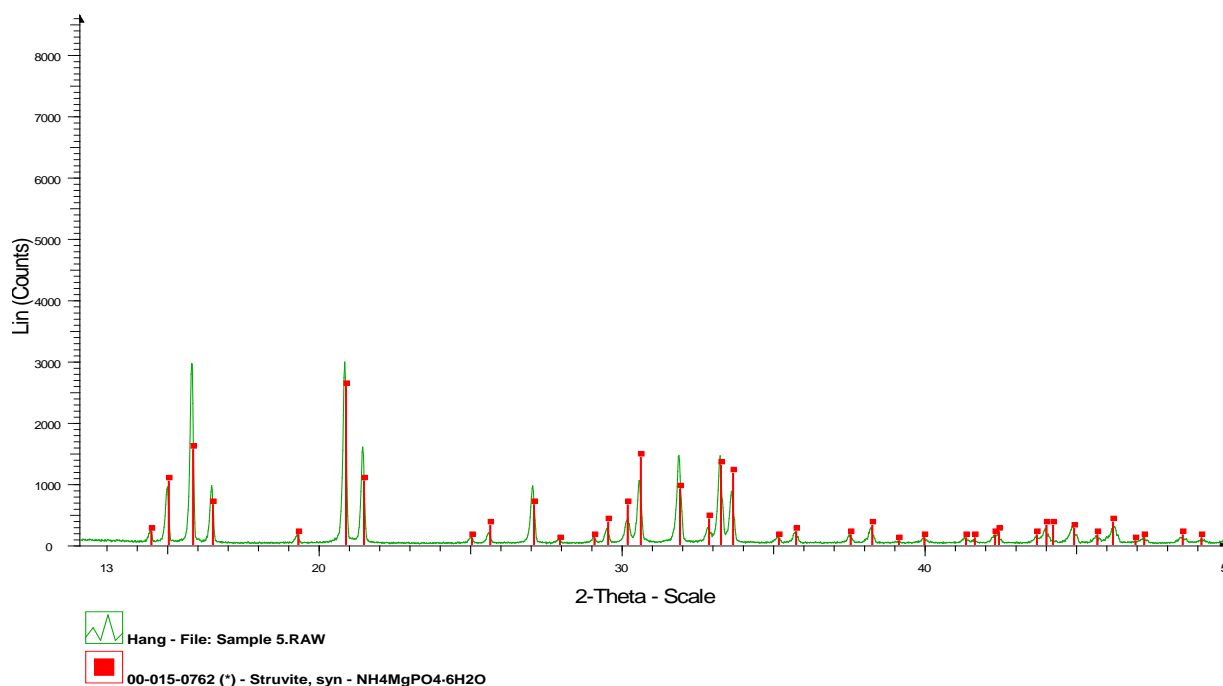


Figure 4. XRD pattern of MAP recovered from phosphorus desorption solution at the optimal crystallization condition.

The morphology of the recovered precipitate was displayed in Figure 5. It can be seen from the figure that the settled solids were orthorhombic crystals with a white color and an average length of 40 μm . In the previous studies, the MAP crystals were found to have orthorhombic, needle-like, and quasi-spherical structures [23]. The average size of MAP crystals varied from 0.25 to 80 μm [39], [41]. The

comparison with earlier studies shows that the recovered precipitate had the typical shape and the medium size of MAP crystals.

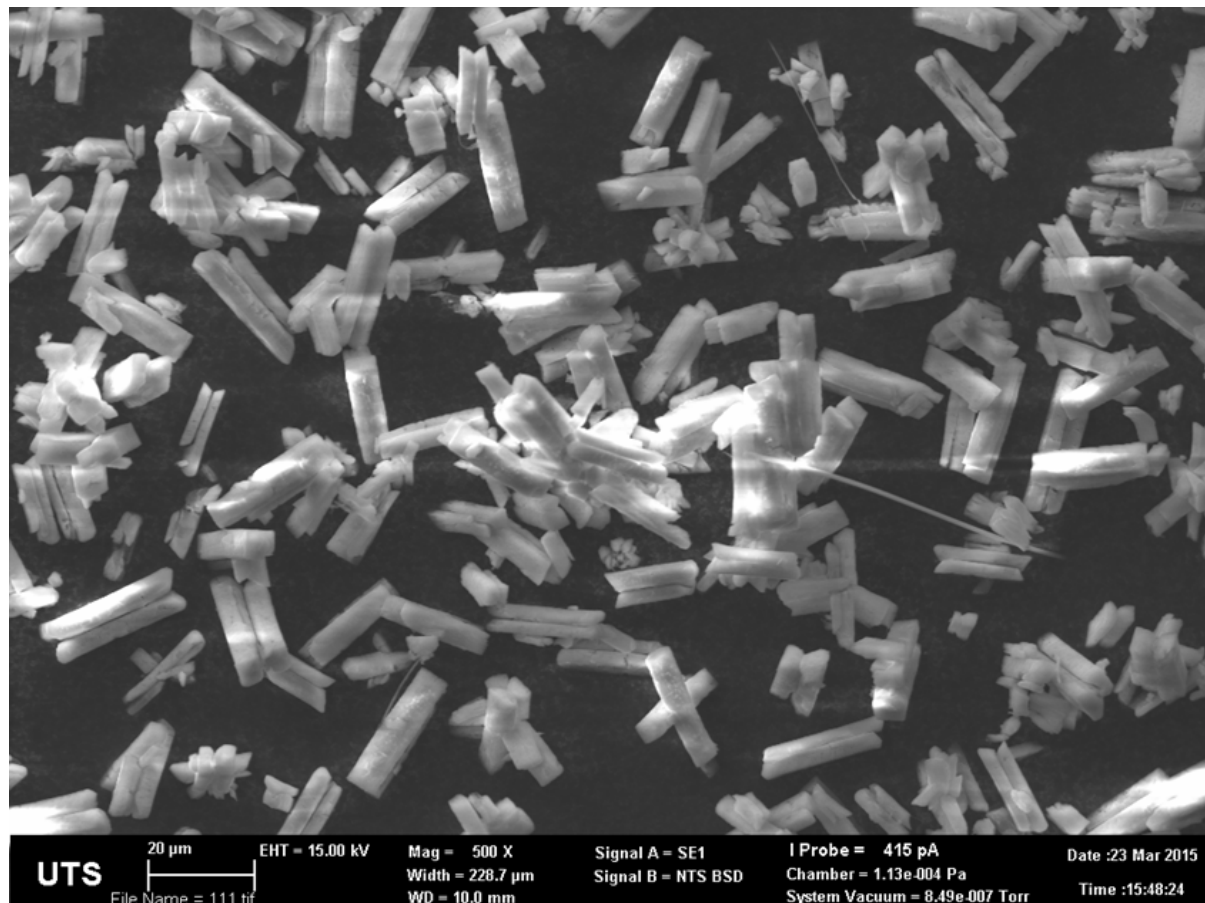


Figure 5. SEM image of MAP recovered from phosphorus desorption solution (pH = 9, Mg: N: P molar ratio = 2:2:1, initial phosphorus concentration = 156 mg/L, stirring speed = 120 rpm, reaction temperature = 295 K).

The FTIR pattern of the reclaimed precipitate was recorded on an IRAffinity-1 FTIR, Shimadzu Corporation (Japan). The peak at 2889.49cm^{-1} represents O-H (very broad) in carboxylic acids and derivatives. The peak at 2343.61cm^{-1} arises from phosphorus functions (P-H phosphine, med & shp). A broad band in the range between 1595.2 and 1581.7cm^{-1} can be assigned to NH_2 scissoring (1° amines) in amines. The band at 1437.03cm^{-1} suggests the presence of C-O-H bending in carboxylic acids and derivatives. The peak at 987.6cm^{-1} is attributed to the P-H phosphine (P-H pending) in phosphorus functions. The bands seen over the range of $885.36\text{--}750.34\text{cm}^{-1}$ correspond to NH_2 and N-H wagging (shifts on H-bonding) in amines. Similar adsorption bands have been observed by [15], and [29] for MAP recovered from different types of wastewater. Based on the obtained IR data, it is confirmed that PO_4 and NH_4 are main components of the recovered precipitate.

In this study, MAP purity was determined according to the minimum molar number of MAP components. Accordingly, 2.48 g of the precipitate recovered at the optimal crystallization condition was dissolved with 1 L of milli-q water. The millimolar numbers of P, Mg, and N were calculated to be 9.58, 9.38, and 9.72, respectively. Thus, the millimolar number of MAP was 9.38, and the percentage of MAP in the precipitate was 92.59%.

The bioavailability of the recovered precipitate is evidenced by its solubility in 2% citric acid [10]. It was found that the citric acid solubility of the harvested precipitate was approximately 89% by mass.

A similar P-bioavailability (94%) was reported by [42] for the MAP recovered from sewage sludge ash. Due to high purity, high P-availability and low contents of heavy metals, the recovered MAP can be used as a high-quality fertilizer.

4. Conclusions

Although the phosphorus recovery as MAP from municipal wastewater has a great potential, it remains a challenge. This work aims at recovering MAP from municipal wastewater by means of adsorption combined with crystallization. The main concluding remarks were drawn from this work as follows:

- A semi pilot-scale ZLO column could pre-concentrate phosphorus from municipal wastewater more than 28 times, providing a sufficiently high phosphorus concentration for MAP recovery.
- The MAP crystallization from phosphorus desorption solution was most favored at the following operating conditions: pH = 9, Mg: N: P molar ratio = 2:2:1, the chemical combination of $\text{MgCl}_2 \cdot 6\text{H}_2\text{O}$ and NH_4Cl , and room temperature.
- The results of XRD, SEM, FTIR, elemental analyses verified that the optimum crystallization conditions resulted in high-quality MAP crystals, with the MAP purity of 92.59%, and the P-availability of 89% by mass. Overall, the combination between adsorption onto ZLO and crystallization as MAP can be a good solution for the phosphorus recovery from municipal wastewater.

Acknowledgements

The authors appreciate Sustainable Water Program – Theme of Wastewater Treatment and Reuse Technologies, Centre for Technology in Water and Wastewater (CTWW), School of Civil and Environmental Engineering, University of Technology, Sydney (UTS) for providing analytical facilities and Australia Awards for granting the scholarship.

References

- [1] Petzet S, Peplinski B and Cornel P 2012 On wet chemical phosphorus recovery from sewage sludge ash by acidic or alkaline leaching and on optimized combination of both *Water Res.* **46** 3769-80
- [2] Karachalios A P 2012 Nutrient removal from water by various quaternized wood agricultural residues using a choline based ionic liquid analogue (Doctoral thesis). Stevens Institute of Technology, New Jersey, United States.
- [3] Choi J, Lee S, Kim J, Park K, Kim D and Hong S 2012 Comparison of surface modified adsorbents for phosphate removal in water *Water Air Soil Poll.* **223** 2881-90
- [4] Eljamal O, Okawauchi J, Hiramatsu K and Harada M 2013 Phosphorus sorption from aqueous solution using natural materials *Environ. Earth Sci.* **68** 859-63
- [5] Xu X, Gao B, Yue Q, Zhong and Q 2011 Sorption of phosphate onto giant reed based adsorbent: FTIR, Raman spectrum analysis and dynamic sorption/desorption properties in filter bed *Bioresour. Technol.* **102** 5278-82
- [6] Kalmykova Y and Fedje K 2013. Phosphorus recovery from municipal solid waste incineration fly ash *Waste Manage.* **33** 1403-10
- [7] Schick J, Kratz S, Adam C and Schnug E 2009 Techniques for P recovery from waste water and sewage sludge and fertilizer quality of P recycling products
http://www.mmm.fi/attachments/mmm/ministerio/5n8h6xg9T/presentation_judith_schick.pdf (accessed 15.04.30)
- [8] Gibbons M K 2009 The use of water treatment residual solids for arsenate and phosphate adsorption (Doctoral thesis). Dalhousie University, Nova Scotia, Canada.
- [9] Mezenner N Y and Bensmaili A 2009 Kinetics and thermodynamic study of phosphate adsorption on iron hydroxide eggshell waste *Chem. Eng. J.* **147** 87-96
- [10] Nieminen J 2010 Phosphorus recovery and recycling from municipal wastewater sludge (Master of Science thesis). Aalto University, Espoo, Finland

- [11] Kumar P, Sudha S, Chand S and Srivastava V C 2010 Phosphate removal from aqueous solution using coir pith activated carbon *Separ. Sci. Technol.* **45** 1463-70
- [12] Namasivayam C and Sangeetha D 2004 Equilibrium and kinetic studies of adsorption of phosphate onto ZnCl₂ activated coir pith carbon *J. Colloid Interf. Sci.* **280** 359-65
- [13] Parsons S and Smith J A 2008 Phosphorus removal and recovery from municipal wastewaters *Elements* **4** 109-12
- [14] Cornel P and Schaum C 2009 Phosphorus recovery from wastewater: needs, technologies and costs *Water Sci. Technol.* **59** 1069-76
- [15] Li H, Ye Z and Wang F 2012 Phosphorus recovery as struvite from eutrophic waters by XDA-7 resin *Water Sci. Technol.* **65** 2091-7
- [16] Sengupta S and Pandit A 2011 Selective removal of phosphorus from wastewater combined with its recovery as a solid-phase fertilizer *Water Res.* **45** 3318-30
- [17] Xu X, Gao B Y, Yue Q Y and Zhong Q Q 2010 Preparation of agricultural by-product based anion exchanger and its utilization for nitrate and phosphate removal *Bioresour. Technol.* **101** 8558-64
- [18] Benyoucef S and Amran M 2011 Adsorption of phosphate ions onto low cost Aleppo pine adsorbent *Desalin.* **275** 231-6
- [19] Karthikeyan K G, Tshabalala M A and Wang D 2002 Use of lignocelluloses materials for sorption media for phosphorus removal. ASAE Annual International Meeting/ CIGR 15th World Congress, Chicago, Illinois, USA, July 28-31.
- [20] Anirudhan T S, Noelin B F and Manohar D M 2006 Phosphate removal from wastewaters using a weak anion exchanger prepared from a lignocellulosic residue *Environ. Sci. Technol.* **40** 2740-5
- [21] Ismail Z Z 2012 Kinetic study for phosphate removal from water by recycled date-palm wastes as agricultural by-products *Int. J. Environ. Studies* **69** 135-49
- [22] Peng F, He P, Luo Y, Lu X, Liang Y and Fu J 2012 Adsorption of phosphate by biomass chars deriving from fast pyrolysis of biomass waste *Clean Soil Air Water* **40**, 493-8
- [23] Karabegovic L, Uldal M, Werker A and Morgan-Sagastume F 2013 Phosphorus recovery potential from a waste stream with high organic and nutrient contents via struvite precipitation *Environ. Technol.* **34** 871-83
- [24] Nguyen T A H, Ngo H H, Guo W S, Zhang J, Liang S, Lee D J, Nguyen P D and Bui X T 2014a Modification of agricultural waste/by-products for enhanced phosphate removal and recovery: Potential and obstacles. *Bioresour. Technol.* **169** 750-62
- [25] Perera P W A, Han Z Y, Chen Y X and Wu W X 2007 Recovery of nitrogen and phosphorous as struvite from swine waste biogas digester effluent *Biomed. Environ. Sci.* **20**, 343-50
- [26] Song Y, Yuan P, Zheng B, Peng J, Yuan F and Gao Y 2007 Nutrients removal and recovery by crystallization of magnesium ammonium phosphate from synthetic swine wastewater *Chemosphere* **69** 319-24
- [27] Okano K, Uemoto M, Kagami J, Miura K, Aketo T, Toda M, Honda K and Ohtake H 2013 Novel technique for phosphorus recovery from aqueous solutions using amorphous calcium silicate hydrates (A-CSHs) *Water Res.* **47** 2251-9
- [28] Bradford-Hartke Z, Lant P and Leslie G 2012. Phosphorus recovery from centralized municipal water recycling plants *Chem. Eng. Res. Design* **90** 78-85
- [29] Nur T 2014 Nitrate, phosphate and fluoride removal from water using adsorption process (Doctoral thesis). University of Technology, Sydney, NSW, Australia
- [30] Nguyen T A H, Ngo H H, Guo W S, Nguyen T V, Zhang J, Liang S, Chen S S and Nguyen N C 2014b A comparative study on different metal loaded soybean milk by-product 'okara' for biosorption of phosphorus from aqueous solution *Bioresour. Technol.* **169** 291-8
- [31] Nguyen T A H, Ngo H H, Guo W S, Zhou J L, Wang J, Liang H and Li G 2014c. Phosphorus elimination from aqueous solution using 'zirconium loaded okara' as a biosorbent *Bioresour. Technol.* **170** 30-7

- [32] Awual Md R and Jyo A 2011 Assessing of phosphorus removal by polymeric anion exchangers *Desalin.* **281** 111-7
- [33] Hao X D, Wang C C, Lan L and van Loosdrecht M C M 2008 Struvite formation, analytical methods and effects of pH and Ca^{2+} *Water Sci. Technol.* **58** 1687-92
- [34] Mallampati R, Liu YH, Kumar S and Kwag J H 2013 Magnesium ammonium phosphate formation, recovery and its application as valuable resources: a review *J. Chem. Technol. Biotechnol.* **88** 181-9
- [35] Ebie Y, Kondo T, Kadoya N, Mouri M, Maruyama O, Noritake S, Inamori Y and Xu K 2008 Recovery oriented phosphorus adsorption process in decentralized advanced Johkasou *Water Sci. Technol.* **57** 1977-81
- [36] Garcia-Belinchón C, Rieck T, Bouchy L, Gali A, Rouge P and Fabregas C 2013 Struvite recovery: pilot scale results and economic assessment of different scenarios *Water Practice Technol.* **8** 119-30
- [37] Çelen I, Buchanan J R and Burns R T 2007 Using a chemical equilibrium model to predict amendments required to precipitate phosphorus as struvite in liquid swine manure *Water Res.* **41** 1689-96
- [38] Wilsenach J A, Schuurbiers C A H and van Loosdrecht M C M 2007 Phosphate and potassium recovery from source separated urine through struvite precipitation *Water Res.* **41** 458-66
- [39] Jia G 2014 Nutrient removal and recovery by the precipitation of magnesium ammonium phosphate (Master of Science thesis). The University of Adelaide, South Australia, Australia
- [40] Le Corre K S, Valsamie J E, Hobbs P and Parsons S A 2009 Phosphorus recovery from wastewater by struvite crystallization: a review *Crit. Rev. Env. Sci. Tec.* **39** 433-77
- [41] Hutnik N, Kozik A, Mazieniczuk A, Piotrowsk K, Wierzbowska B and Matynia A 2013. Phosphates (V) recovery from phosphorus mineral fertilizers industry wastewater by continuous struvite reaction crystallization process *Water Res.* **47**, 3635-43
- [42] Xu H, He P, Gu W, Wang G and Shao L 2012 Recovery of phosphorus as struvite from sewage sludge ash *J. Environ. Sci.* **24** 1533-8